Click Here for Full Article

Influence of coarse lag formation on the mechanics of sediment pulse dispersion in a mountain stream, Squire Creek, North Cascades, Washington, United States

Chris J. Brummer[1] and David R. Montgomery[1]

Received 2 December 2005; revised 11 March 2006; accepted 4 April 2006; published 21 July 2006.

[1] Mountain channels closely coupled to landslide-prone hillslopes often exhibit bed surface grain sizes coarser than transportable by annual high flows. Coarse particles within poorly sorted sediment delivered to channels by mass-wasting processes may not be readily transported as bed load and can consequently form lag deposits that influence the morphology, hydraulic roughness, and sediment storage within mountain channel networks. A tracer study and comparison of supply and bed grain size distributions from a valley-spanning landslide in the North Cascades of Washington state were used to derive relations between shear stress and the probability of particle entrainment and erosion from the sediment pulse. Rapid bed surface armoring formed a relatively immobile lag deposit within 2 years. Covering of 20% of the bed by lag boulders with <5% probability of entrainment was sufficient to retard vertical incision and force considerable channel widening during a flood with an 8- to 152-year recurrence discharge on locally gauged streams. Our results imply that numerical models of sediment pulse evolution that do not explicitly incorporate the influence of lag formation may substantially overestimate long-term dispersion rates. The grain size distribution and lithology of a sediment input relative to the flow competence of the receiving channel are important factors influencing the rates and mechanisms of sediment pulse dispersion and the sediment capacitance provided by coarse-grained sediment pulses in mountain drainage basins.

Citation: Brummer, C. J., and D. R. Montgomery (2006), Influence of coarse lag formation on the mechanics of sediment pulse dispersion in a mountain stream, Squire Creek, North Cascades, Washington, United States, *Water Resour. Res.*, *42*, W07412, doi:10.1029/2005WR004776.

1. Introduction

[2] Sediment supply from mass wasting dominates the storage and routing of sediment in confined, steep gradient mountain channels [*Dietrich and Dunne*, 1978; *Caine and Swanson*, 1989; *Benda*, 1990]. Episodic sediment inputs characteristic of mountain streams can create pulses that translate downstream as a coherent wave or disperse in place. General controls on sediment wave behavior are important for understanding the geomorphology and ecology of mountain streams. Recent theoretical and experimental studies suggest that sediment pulses in rivers with high subcritical flood Froude numbers will decay in place by dispersion [*Cui et al.*, 2003a, 2003b], whereas downstream translation is favored in sand-bedded channels with relatively low Froude numbers and when the introduced sediment is finer than the ambient bed material [*Lisle et al.*, 1997; *Wohl and Cenderelli*, 2000; *Cui et al.*, 2003a, 2003b]. *Sutherland et al.* [2002] applied the numerical model developed by *Cui et al.* [2003a, 2003b] to the degradation of a landslide that entered the Navarro River in northern California and found that the model results agreed well with field measurements documenting the dispersive evolution of the river bed to near its original profile within four years. However, as *Lisle and Church* [2002] note, the bed load transport function in the model does not account for bed forms or cellular particle structures that might form from the reworking of coarse-grained sediment. Here we investigate a coarse-grained sediment pulse resulting from an instantaneous input of poorly sorted sediment containing a significant fraction of coarse particles too large to be transported as bed load by typical high flows. Although coarse-grained sediment pulses triggered by landslides are common in tectonically active regions, and their morphologic effects have received considerable attention [e.g., *Costa and Schuster*, 1991; *Schuster et al.*, 1992; *Pringle et al.*, 1998; *Korup*, 2004, 2005; *Ouimet and Whipple*, 2004], the rates and mechanisms by which mountain channels assimilate coarse-grained sediment pulses are poorly understood.

[3] The morphology of alluvial channels in mountain drainage basins varies systematically with gradient to produce a stable roughness configuration that balances transport capacity with sediment supply [*Montgomery and Buffington*, 1997]. Adjustments to bed surface texture can occur across a broad range in channel gradient [*Kinerson*, 1990; *Lisle*, 1995; *Brummer and Montgomery*, 2003]. However, variations in form roughness and slope arising from lateral migration and adjustments in sinuosity are the primary regulators of sediment transport capacity in most

[1]Department of Earth and Space Sciences, University of Washington, Seattle, Washington, USA.

Copyright 2006 by the American Geophysical Union.
0043-1397/06/2005WR004776$09.00

low-gradient floodplain channels [*Schumm*, 1963; *Leopold et al.*, 1964]. In contrast, valley confinement in steep gradient channels (slopes greater than about 0.03) favors the adjustments of bed surface texture through armoring and the organization of the coarsest particles into characteristic, energy-dissipating structures. For channel gradients ranging from about 0.03 to 0.10, the coarsest particles are commonly organized into a sequence of channel-spanning steps and pools that promote bed stabilization through the maximization of resistance to flow [*Whittaker and Jaeggi*, 1982; *Abrahams et al.*, 1995]. Step spacing has also been found to correspond with antidunes and the theoretical wavelength of standing waves, under which large clasts come to rest during transient conditions of critical flow [*Whittaker and Jaeggi*, 1982; *Grant*, 1997; *Chartrand and Whiting*, 2000]. However, large particles exhumed during the fluvial reworking of coarse-grained sediment pulses and exhibiting mobility thresholds that exceed typical high flows can dominate the bed surface texture of confined channels. For example, *Zimmerman and Church* [2001] found support for neither the flow resistance nor the antidune hypothesis for step-pool formation. They attributed the highly variable step wavelength observed in their study reaches to the semirandom placement of stable boulders supplied by mass wasting. The authors found that steps destroyed by floods reformed around stationary keystones. Likewise, in their laboratory flume, *Curran and Wilcock* [2005] observed a random spacing of steps and found no support for grain deposition beneath water surface waves. *Montgomery and Buffington* [1997] concluded that the disorganized arrangement of coarse particles in some cascade-type channels represents stable lag deposits forced by mass wasting. It follows that the size distribution of sediment supplied to mountain channels by mass-wasting processes should influence bed stability and the configuration of energy dissipating structures and thereby potentially moderate the dispersion of coarse-grained sediment pulses.

[4] The self-stabilizing tendency of alluvial channels imposes a threshold for bed mobilization that varies with position in the channel network. Bed stabilization by surface armoring of poorly sorted sediment is well documented in low-gradient channels under conditions of excess sediment transport capacity [*Dietrich et al.*, 1989; *Church et al.*, 1998; *Buffington and Montgomery*, 1999; *Lisle and Church*, 2002]. Decades of work on gravel bed channels has established the generality of a threshold for armor mobility corresponding to discharges at or below bankfull flow, which typically occurs roughly every 1.5 to 2 years based on flood frequency analyses [*Wolman and Miller*, 1960; *Andrews*, 1980; *Whiting et al.*, 1999]. Higher up in the channel network, studies of step-pool formation following channel disturbance document rapid bed stabilization by typical flows and a progressive increase in the threshold for step reorganization corresponding to flows with a recurrence interval of about 20–50 years [*Grant et al.*, 1990; *Lenzi*, 2001; *Madej*, 2001; *Kasai et al.*, 2004; *Chin and Wohl*, 2005]. The disorganized arrangement of lag boulders in many cascade channels suggests a stable morphology between bed-resetting debris flows, which have recurrence intervals of 10^2–10^3 years depending on the relative stream order [*Benda*, 1990]. The overlap in channel gradient for the occurrence of cascade and step-pool morphologies may reflect the variability in supply caliber with respect to the largest particle that can be transported by typical high flows (i.e., the flow competence of the stream). Hence lag deposits represent the stable end-member of the continuum of mobility thresholds observed in many alluvial channels.

[5] Although the high threshold for bed mobility in steep mountain channels is widely recognized, the mechanisms of armor formation in these steep channels remain poorly understood. Previous work in debris flow-dominated channels shows a stream power dependence on armoring even for steep (lag prone) channels [*Brummer and Montgomery*, 2003]. Lag development in steep gradient channels implies that armoring may also be forced by the selective transport of sediment supplied by mass wasting. *Lisle and Church* [2002] examined sediment transport-storage relations using flume experiments, numerical simulations, and field examples of degrading channels. They found a rapid decline in transport rate and depth of incision in response to armoring and surface structure development. The effect was greatest in poorly sorted material. Selective transport should also be more pronounced and lead to lag formation where the coarse tail of the supply distribution exceeds the competence of typical high flows. Lag development that shields coarse-grained sediment pulses from incision can form sediment reservoirs in headwater channels and moderate the dispersion of sediment inputs within mountain channel networks.

[6] Lag formation in steep-gradient channels may have particular importance for the understanding of how channels process coarse-grained sediment pulses, as field studies to date have focused on sediment pulses derived from source rocks that supply particle distributions readily transported by typical flows [*Gilbert*, 1917; *Roberts and Church*, 1987; *Perkins*, 1989; *Madej and Ozaki*, 1996; *Wohl and Cenderelli*, 2000; *Sutherland et al.*, 2002; *Cui et al.*, 2003a, 2003b]. Because a boulder lag may inhibit the erosion of the mass-wasting deposit from which it evolves, an assessment of the mobility of large particles is necessary to understand the dispersion rate and residence time of coarse-grained sediment pulses in mountain channel networks. We use the case study of a coarse-grained bedrock landslide and valley-spanning debris dam in the North Cascades of Washington to investigate lag formation and attendant effects of sediment capacitance in a mountain stream.

2. Study Area and Landslide Description

[7] A massive landslide in the Squire Creek basin on 25 February 2002 created a sediment pulse that temporarily blocked the creek. The study area is located 3.5 km southwest of the town of Darrington in the north Cascades of Washington (Figure 1). Elevations within the basin range from about 130 m at the confluence with the North Fork Stillaguamish River to 2090 m on Three Fingers Peak. Most of the basin is underlain by granitic rocks of the Squire Creek stock. Fault-bounded, ultramafic rocks of the Darrington-Devils Mountain Fault Zone [*Tabor et al.*, 2002] form the ridge north of Jumbo Mountain, where the landslide originated. Recessional outwash deposits form terraces in the lower reach of Squire Creek and within the study area.

[8] The basin receives an average of 2000–3400 mm of annual precipitation, which falls primarily between October and March as rain [*Daly and Taylor*, 1998]. Snow accumu-

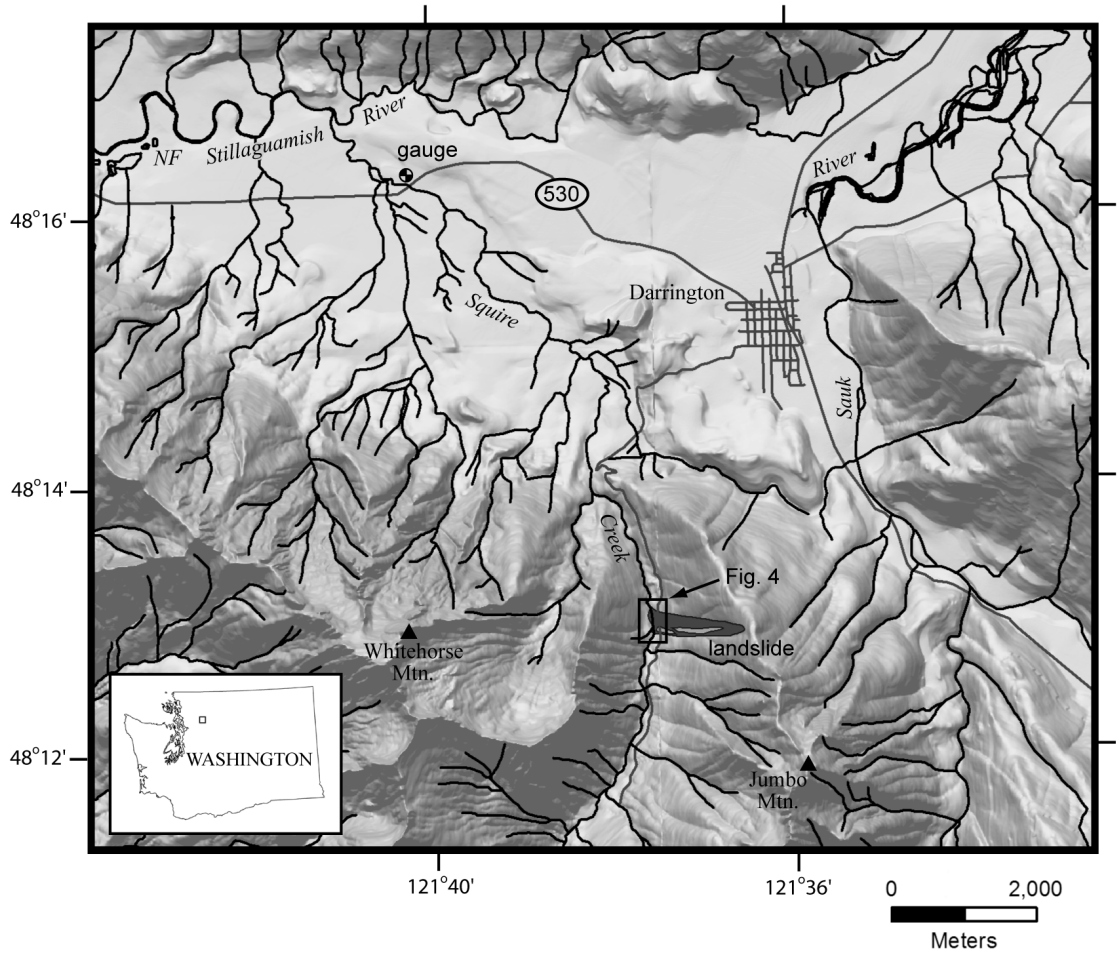

Figure 1. Shaded relief map of the Squire Creek area showing the landslide, channel network, and gauging station.

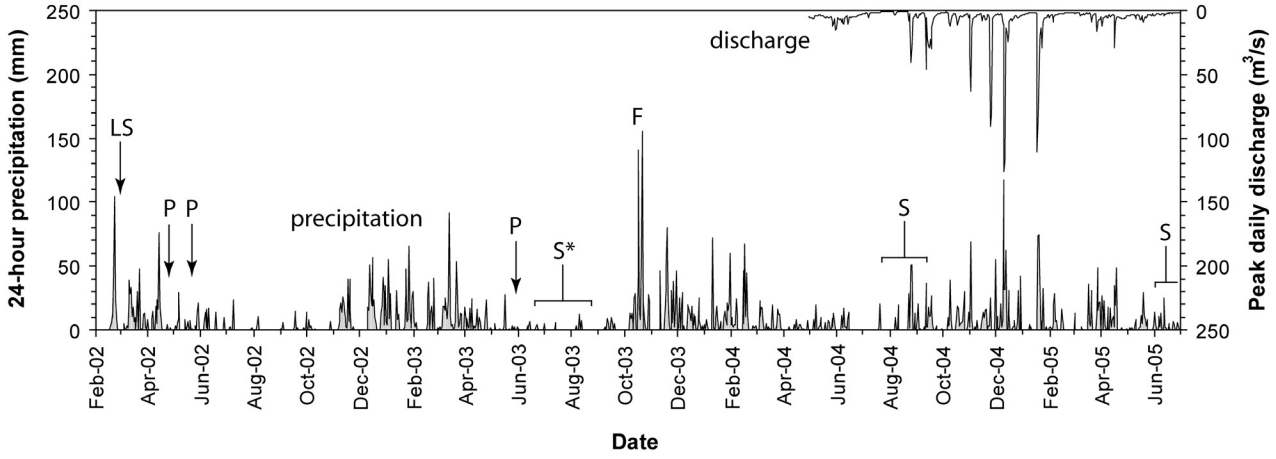

Figure 2. Daily precipitation (Darrington Ranger Station) and streamflow at the highway 530 bridge (Washington Department of Ecology, Squire Creek at Squire Creek Park, gauge 05H070). Missing precipitation obtained from correlation with the Concrete PPL Fish Station ($y = 1.05x$, $r^2 = 0.48$). Notation indicates dates of the landslide (LS), photo documentation (P), field surveys (S, asterisk denotes pebble counts), and the 16–21 October 2003 floods (F).

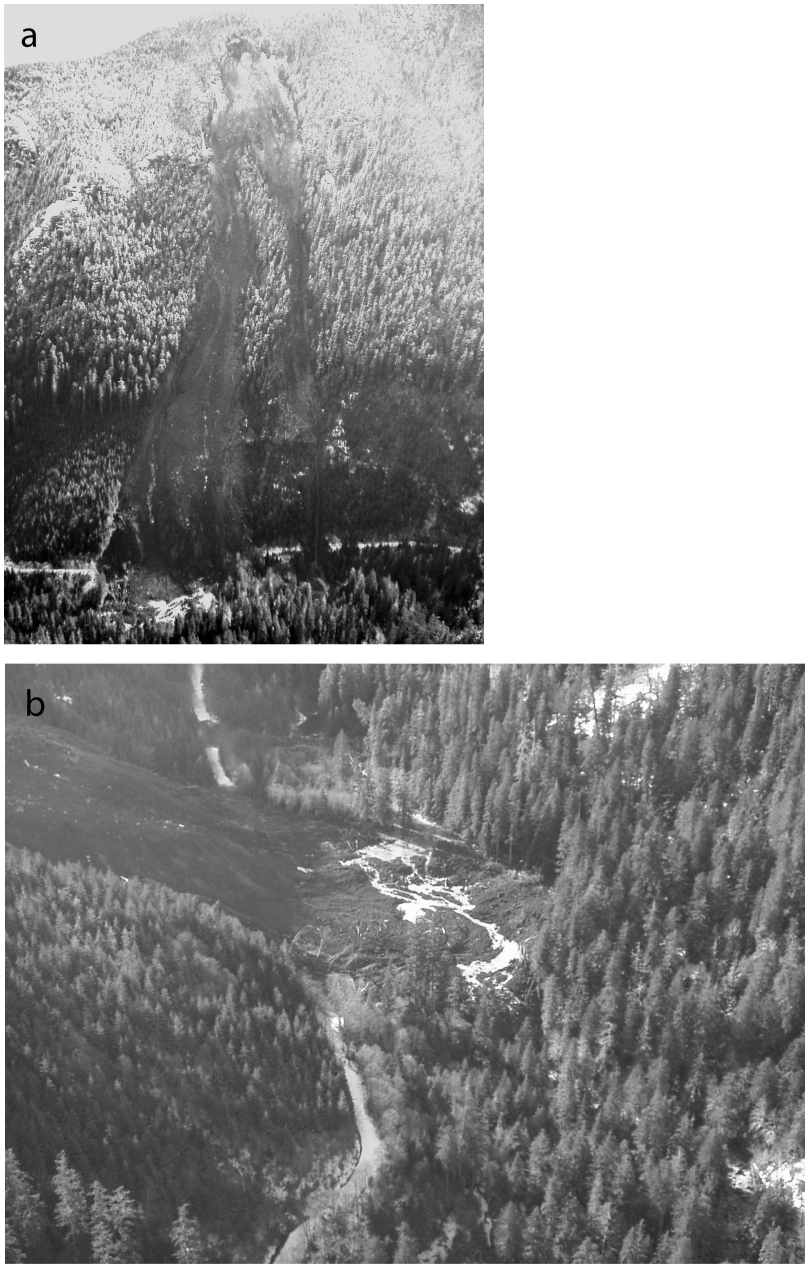

Figure 3. Oblique aerial photographs taken 2 hours after the landslide: (a) the 1500-m runout and (b) water flowing over the landslide dam, view looking upstream (photographs by R. Hausinger, U.S. Forest Service).

lation occurs throughout the basin but typically melts by late summer even at the highest elevations. Squire Creek has been gauged approximately 8.8 km downstream of the landslide at the highway 530 bridge by the Washington State Department of Ecology since May 2004. Streamflow is dominated by storm runoff and responds within hours to precipitation. The majority of the basin is vegetated with old growth, conifer forest, although northern portions of the valley bottom and the base of eastern slopes were logged as recently as the 1980s. These areas are densely vegetated with a second-growth, mixed deciduous and conifer forest.

[9] At the landslide deposit, Squire Creek drains a basin area of 26.0 km^2. Adjacent reaches of Squire Creek unaffected by the landslide have a mean gradient of 0.08 and average bankfull width of 23 m. The study reach is a step-pool channel [*Montgomery and Buffington*, 1997] containing large boulders, some with diameters exceeding the bank height by several meters. Except for a short channel reach approximately 700 m below the study area, bedrock is not exposed in the valley bottom, and the channel is formed entirely within sediment derived from glacial outwash, mass wasting, and recent fluvial processes. Aside from the recent landslide, extensive field reconnaissance and examination of aerial photographs found no evidence of significant historical (i.e., <100 years) slope failures in the basin.

[10] The Squire Creek landslide occurred after a series of moist Pacific frontal systems delivered over 200 mm of precipitation in a week (Figure 2), as recorded at the

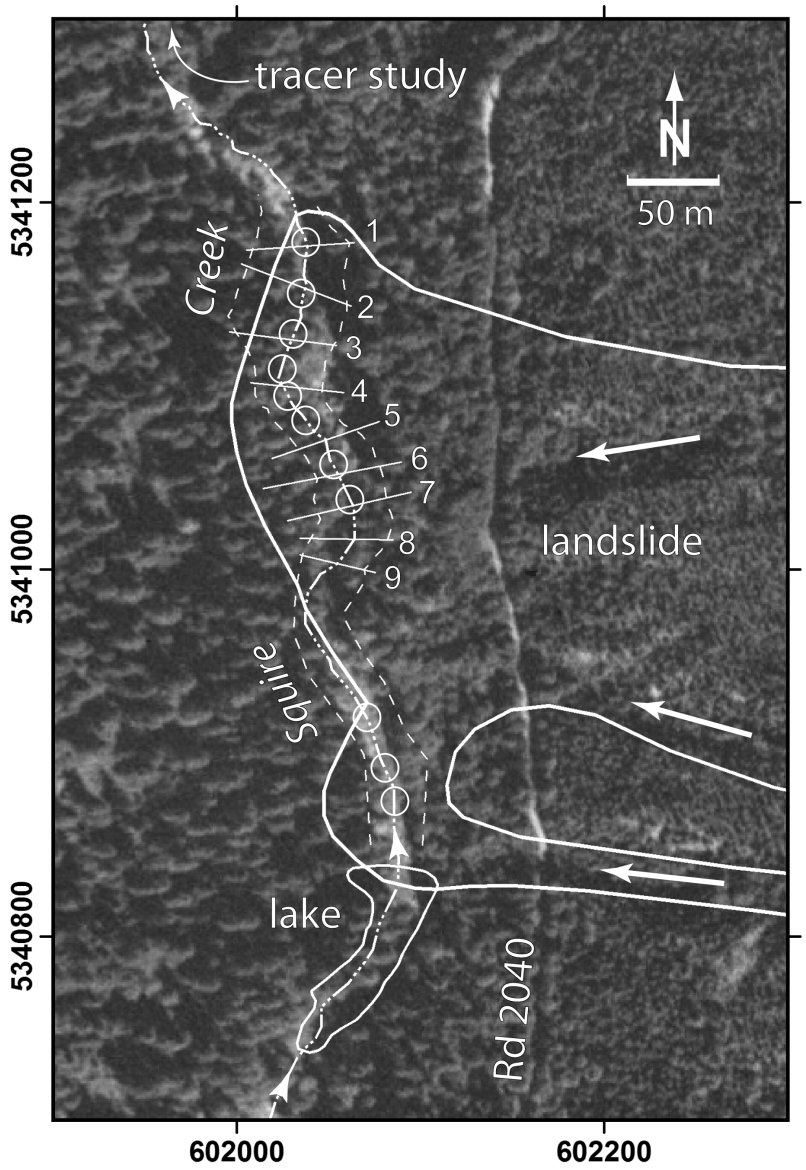

Figure 4. Overlay of landslide toe and 1989 USGS orthophoto (WA State Plane N. NAD83, meters) showing the landslide perimeter and backwater lake (solid lines), thalweg, top of bank surveyed in 2004 (dashed lines), location of cross sections (1–9), the 11 bed surface sampling locations for the MB model (circles), and the tracer study. Arrows on landslide surface depict flow direction in bedrock ravines.

Darrington Ranger Station (elevation of 167 m, mean annual precipitation 2020 mm). The failure began as a deep-seated rock avalanche from the ridge north of Jumbo Mountain and evolved into two debris flow tracks as it entrained soil and woody debris during the 1500-m descent to the valley bottom (Figure 3). An estimated 125,000 m^3 of rock, soil, and wood were deposited along a 400-m reach of the valley floor (elevation of 360 m) and temporarily dammed Squire Creek. Video recorded from a U.S. Forest Service helicopter approximately two hours after the event shows formation of a backwater lake and a multithread channel traversing the landslide dam (Figure 3).

3. Methods

[11] Postlandslide modification of the bed surface grain size distribution was measured using grid-by-number particle counts [*Wolman*, 1954]. Particle counts were conducted at nine locations on the undisturbed surface of the landslide deposit and combined into a composite grain size distribution (942 point counts). Reach average particle counts (>100 counts each) were conducted on the channel bed through the landslide deposit at 11 locations (Figure 4). Particle counts were conducted across the entire high-flow channel width and along a reach length roughly equivalent to one channel width. Fluvial incision through the landslide deposit was documented by repeated field surveys of the channel profile and cross sections. Field work was conducted during summer 2003, 2004, and 2005, whereas photographs compiled from field reconnaissance by others document early channel evolution before 2003. A longitudinal profile of the channel thalweg was constructed in 2003 by surveying every step and pool feature along ~1 km of

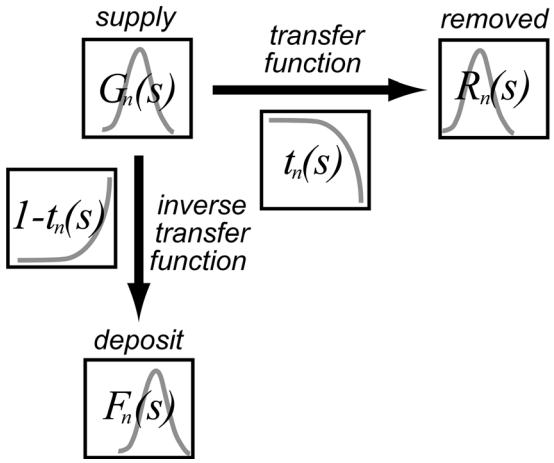

Figure 5. Schematic illustration of the McLaren and Bowles model. Boxes show the generalized frequency distributions of the log-transformed grain size distribution for the supply ($G_n(s)$), removed sediment ($R_n(s)$), deposit ($F_n(s)$), and transfer function ($t_n(s)$).

the creek. The survey was conducted with a tape, hand level, and stadia rod. In addition, nine cross sections were established and surveyed in summer 2003 between rebar end markers spaced along the creek segment impacted by the landslide. The profile and cross sections were resurveyed in summer 2004 and 2005. Both the perimeter and surface topography of the landslide deposit were surveyed in greater detail in 2004 using a total station theodolite. The original landslide surface above the channel was inferred from photographs taken the day of the landslide and by projecting the surface topography across the top of the channel. The initial volume of the landslide deposit within the valley bottom was calculated from the surface area of the landslide and the average depth of the deposit estimated from the height of exposed channel banks and topographic relief along the landslide perimeter. The volume of material eroded between surveys was calculated by interpolating between cross sections.

[12] Lag formation was documented by comparing transport capacity with the grain size distribution of sediment supplied by the landslide. We derived empirical relationships for the maximum mobile grain size transported by winter flows (D_{max}) using two independent approaches: (1) a tracer study of angular clasts derived from the landslide dam and (2) a probabilistic model of sediment entrainment derived from the difference between grain size distributions of the sediment input (composite of nine pebble counts on the landslide surface) and the creek bed (the 11 in-channel pebble counts of the lag deposit).

[13] Hydrologic data for Squire Creek were compiled from 24-hour historical precipitation data recorded at the Darrington Ranger Station. Gaps in the Darrington record were filled using daily precipitation from the Concrete Fish Station, located 33 km north of Darrington. The Concrete data were adjusted using a linear regression of historical daily precipitation from both sites. Because flow data were not available prior to May 2004, we used the 24-hour precipitation from the nearest recording station in Darrington as a proxy for relative discharge.

3.1. Tracer Study

[14] The relative stability of bed surface material supplied by the landslide was evaluated by tracking angular particles downstream from the landslide for up to 2 km. Particles presumed to have been supplied from the landslide were readily identified by an unweathered appearance, angular shape, and metagabbroic lithology unique to the landslide source area. Stationary particles abrading in place were identified by fluted, faceted, and potholed surfaces sculpted by impacts from fine sediment suspended in flow separation eddies [*Whipple et al.*, 2000; *Springer et al.*, 2005]. In contrast, angular clasts transported downstream from the landslide deposit were considered mobile. At each sample location, we measured the intermediate diameters of all angular metagabbro clasts, as well as clasts on the bed surface that exhibited evidence of long-term stability and in-place abrasion (i.e., fluting and potholing); all angular and fluted clasts larger than ~20 cm were sampled. Local channel slope (S) was calculated from surveyed elevations of the channel bed at upstream and downstream ends of each sample reach. We also measured the channel depth (h) corresponding to seasonal high flow. Because most of the sample reaches lacked a true floodplain, high-water indicators such as vegetation patterns, stain lines, and the height of snagged debris were used to approximate the flow depth corresponding to seasonally high flow in floodplain channels. Total reach average shear stress ($\tau = \rho g h S$) was used as a proxy for tractive forces acting on the bed, where ρ is the density of water and g is gravitational acceleration. Form drag from steps and large boulders was not quantified but could reasonably account for a large fraction of the total shear stress estimated from the depth-slope product. A discriminant function analysis was used to derive the best fit relation between groups of stable and mobile sediment sizes as a function of total shear stress.

3.2. Probabilistic Model

[15] We used a modification of the sediment-trend model first described by *McLaren and Bowles* [1985] to derive empirical relationships between total shear stress, grain size, and the probability of sediment entrainment and transport from the landslide deposit (Figure 5). The McLaren and Bowles (MB) model relates the grain size distribution of the source ($G(s)$) to the distribution of the removed or eroded sediment ($R(s)$) by introducing a transfer function ($t(s)$):

$$t(s_i) = \frac{R(s_i)}{G(s_i)} \tag{1}$$

where $G(s_i)$ and $R(s_i)$ are the proportion of sediment in the ith interval of the grain size distribution (s), and $t(s_i)$ is the transfer coefficient for sediment in the ith grain size interval. The transfer coefficient is also the probability that a particle in the ith grain size interval will be removed from $G(s_i)$. For a poorly sorted $G(s)$ containing clasts exceeding the flow competence, the MB model predicts that the transported sediment will become finer than the source, and the remaining sediment distribution will coarsen and form a lag deposit ($F(s)$). A general solution for the transfer function can be derived from field measurements of the source and bed surface distributions without the need to characterize the distribution of the eroded sediment, where

the sampling of coarse bed load is impractical due to the size of large boulders transported by infrequent, high-intensity floods.

[16] In a closed system, conservation of mass requires that the grain size distribution of removed sediment equals the difference between distributions of the source and lag such that

$$R(s) = G(s) - F(s) \tag{2}$$

Combining equations (1) and (2) yields a solution for the transfer function in terms of the source and lag distributions, which we could readily measure:

$$t(s) = 1 - \frac{F(s)}{G(s)} \tag{3}$$

[17] The MB model has been used primarily to infer transport direction of fine sediments in coastal environments based on the relationships between grain size distributions of sequential deposits [*McLaren and Bowles*, 1985]. *Sutherland* [1987] conceptualized a similar model for gravel bed channels to describe the changes that occur in sediment distributions as bed surface armoring progresses. *Sutherland* [1987] combined eroded and armor distributions to posit a probability of removal for each particle size, which is equivalent to the transfer function in the MB model. To our knowledge, our comparison of residual (lag) deposits to their source size distribution represents the first application of such a model to the quantitative evaluation of bed surface armoring from lag development in mountain channels.

[18] Grain size distributions were developed from normalized particle counts of the landslide deposit ($g(s)$) and the n = 11 particle counts of the bed surface ($f_n(s)$). Particle counts for the probabilistic model were conducted in summer 2003. Grain size was characterized using the logarithmic ψ scale, where ψ and the traditional ϕ scale are related to the median grain diameter (D) in mm by

$$\psi = -\phi = \log_2(D) \tag{4}$$

The intermediate diameter of grains between 2ψ and 12ψ were measured with a graduated ruler or stadia rod to the nearest 0.5ψ interval.

[19] Because only particles coarser than 2ψ (4 mm) were sampled, we had to account for the volume fraction of sediment finer than 2ψ and the volume of the voids in the landslide deposit. The combined volume occupied by voids and sediment $<2\psi$ within the landslide (p) was calculated from the weight of coarse sediment sampled from a known volume of landslide material. The in situ volume was measured from the dimensions of an excavation on the surface of the landslide. Sediment $<2\psi$ was sieved in the field and discarded. The remaining sediment, which was coarser than 2ψ, was air dried on tarps and weighed in the field. The combined volume occupied by voids and sediment $<2\psi$ is given by the constant p calculated from

$$p = 1 - \frac{M_c}{\rho_s V_t} \tag{5}$$

where M_c is the mass of sediment $>2\psi$ (167 kg), ρ_s is the assumed sediment density (2700 kg/m^3), and V_t is the total volume of the excavation (0.095 m^3). Solving equation (5) for p yields a volume fraction of the landslide occupied by both voids and sediment $<2\psi$ of 0.35.

[20] Because the composition of the lag deposit should vary with incision depth, we desired to know the number of grains, by size interval, within the initial source volume above a unit area of the bed from which each lag deposit was derived. Likewise, we also desired to know the number of grains per unit area of the bed surface and the total number of grains in each size interval per unit volume of the supply, which was calculated by converting the grid-by-number particle count of the source distribution to synthetic volume-by-number distributions ($G_n(s)$) for each of the 11 sample locations:

$$G_n(s) = g(s)k_1(1-p)h_n\left(1/D^3\right) \tag{6}$$

where h_n is the incision depth at the nth sample location, D_i is the grain diameter in mm of each size interval, and k_1 is a scaling coefficient in the power law relation between the grid-by-number and volume-by-number distributions such that

$$1 = \frac{(1-p)h_n}{\sum_{i=1}^{21} G_n(s_i)(4/3)\pi(D_i/2)^3} \tag{7}$$

[21] The coefficient k_1 scales the volume-by-number conversion of the grain size distribution (denominator in equation (7)) to the unit volume of the eroded sediment. Equations (6) and (7) were solved simultaneously to obtain a value of 1.91 for k_1 and solution for $G_n(s)$. The total number of grains in each size class per unit area of the channel bed was calculated by converting the grid-by-number particle counts of the bed surface to synthetic area-by-number grain size distributions ($F_n(s)$) for each sample location:

$$F_n(s) = f_n(s)k_2\left(1/D^2\right) \tag{8}$$

where k_2 is a second scaling factor (1.27), similar to k_1, such that the area-by-number conversion equals a unit area of 1 or

$$1 = \sum_{i=1}^{21} F_n(s_i)\pi(D_i/2)^2 \tag{9}$$

In contrast to the volume-by-number conversion, voids and fine sediment need not be accounted for in the surface calculations because an area-by-number sampling surface will always be intersected by the projection of a grain within the surface layer.

[22] Transfer coefficients were derived for the 11 sample locations by combining equation (3) with the synthetic grain size distributions calculated for $F_n(s)$ and $G_n(s)$ in equations (6) and (8), respectively:

$$t_n(s) = 1 - F_n(s)/G_n(s) \tag{10}$$

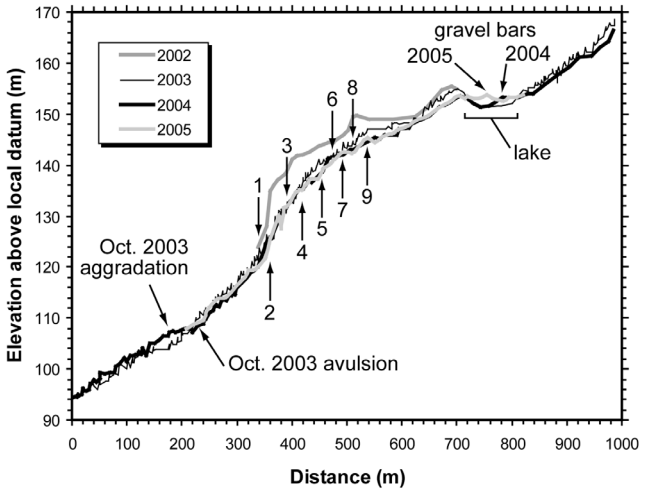

Figure 6. Channel profile through the landslide deposit showing the location of cross sections (1–9), the landslide-dammed lake, the estimated preincision landslide surface in 2002, and the 2003, 2004, and 2005 surveys.

The coarse tails of the transfer functions were truncated at the grain size interval in which $F_n(s) > G_n(s)$ resulted in a negative transfer coefficient. Negative transfer coefficients occur when the number of grains in a unit area of the bed within a particular size interval exceeds the number of grains in the original source volume above that unit area. Although negative transfer coefficients are not possible in a closed system, they occurred in the coarse tails of the distribution because of the small sample population within the coarsest grain size intervals.

[23] Relations between the form of each transfer function and corresponding shear stress were used to develop an empirical model for the probability of sediment entrainment from the landslide deposit as a function of grain size and total shear stress. An analytical solution derived from results of the field sampling (described later) was chosen that minimized residuals between the model and field-based transfer coefficients.

4. Results

[24] The longitudinal profile of Squire Creek exhibits a distinct convexity along the channel reach affected by the landslide (Figure 6). Exposure of a buried forest floor and soil on a relict landslide diamicton beneath the recent landslide deposit indicates that the profile convexity is the result of at least two landslide events. The profile convexity increases the channel gradient at the downstream inflection and reverses the channel gradient at the upstream inflection. Cross sections constructed from field surveys show that the maximum vertical incision occurred directly above the downstream inflection (cross section 2, Figure 7), where the initial channel gradient through the landslide was steepest. During field surveys, we found the bed surface of nearly the entire study reach organized into a coherent step-pool morphology, with most steps spanning the entire channel width (Figure 8). The largest step was over 4 m high and formed a deep plunge pool above cross section 2 (at station 365, where stationing is in m and increases upstream) and near the toe of the landslide deposit. The deposition of intermediate-size material eroded from the landslide formed a boulder bar immediately downstream of the landslide toe between stations 200 and 320. Additional material eroded from the landslide during winter 2003–2004 aggraded the channel farther downstream and forced a channel avulsion at station 230.

[25] A reversal in profile gradient at the upstream inflection formed a backwater lake, which began aggrading at the lake inlet with sand and gravel supplied from upstream. Field observations indicate that at moderate discharge, a portion of the flow overtops the shallow banks at the downstream end of the lake (station 720) and flows through the forest and around the western perimeter of the landslide before rejoining the main stem at station 600. The bifurcation of flow and shallow channel depth at the lake outlet apparently limits vertical incision and the potential for reworking the bed along this upper reach.

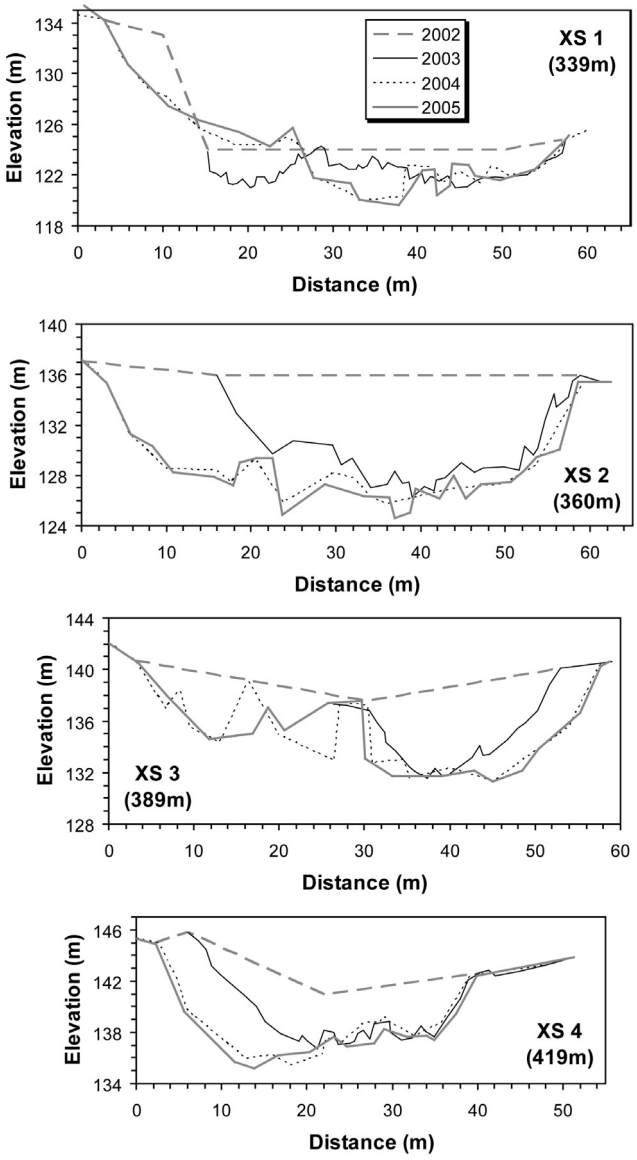

Figure 7. Channel cross sections surveyed in 2003, 2004, and 2005.

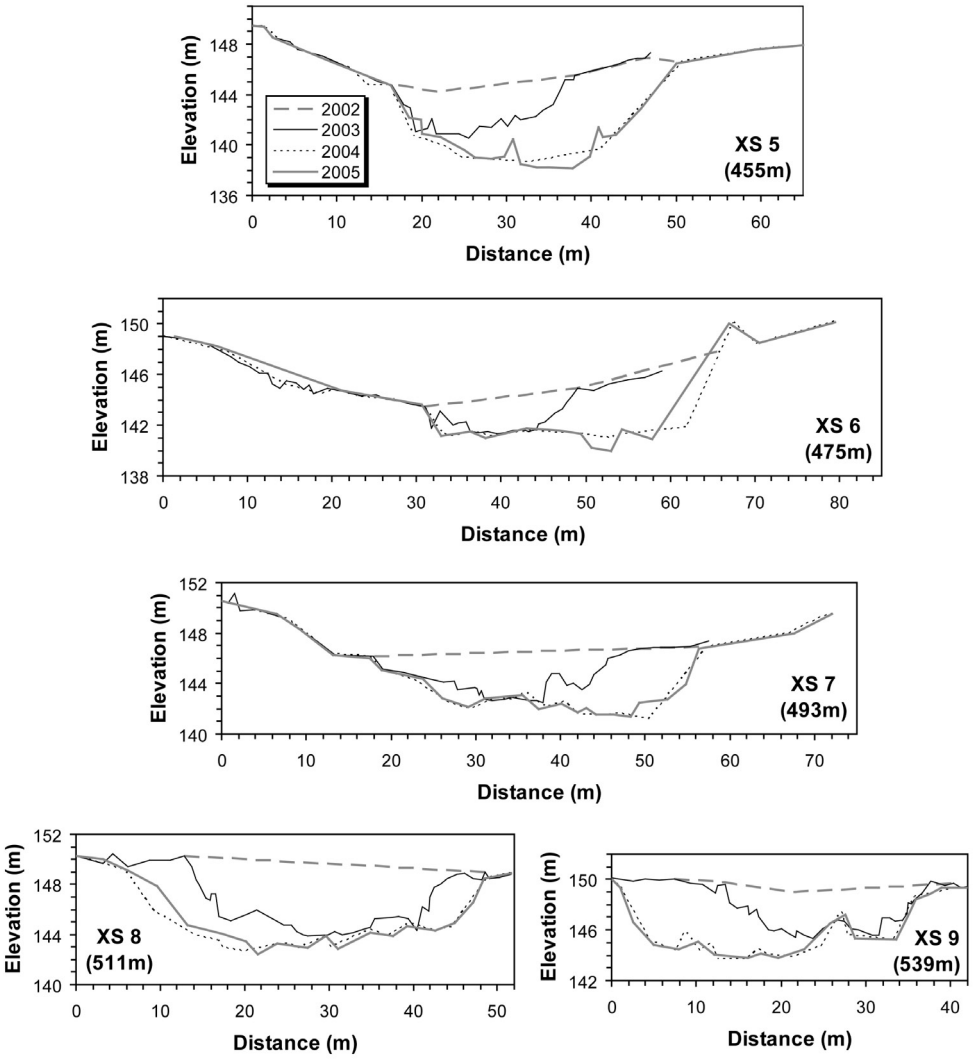

Figure 7. (continued)

Figure 8. Photograph of the creek (summer 2003) between cross sections 5 and 8 showing ~6 m of vertical incision, bed surface armoring, and incipient step-pool morphology.

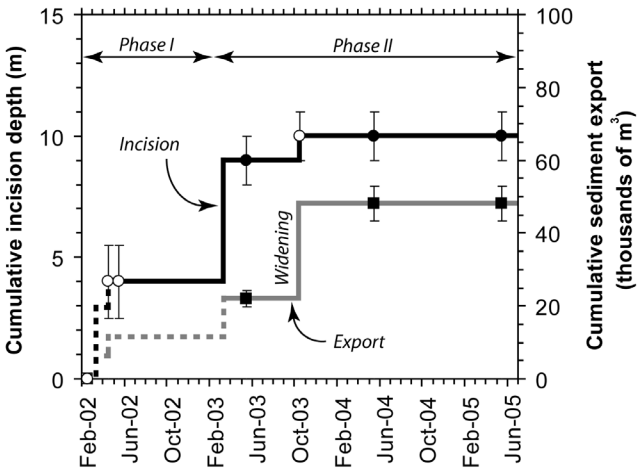

Figure 9. Time series of cumulative channel incision and sediment export constructed from photo documentation (open symbols) and field surveys (solid symbols). Lines are dashed where quantities are inferred. Error bars for the surveyed incision depth correspond to the D_{90} ($\sim$1 m) or more for photointerpreted incision and 10% for sediment volume. Stepped increases in temporal trends correspond to storm events of increasing magnitude (Figure 2), which is supported by our field observations of bed reorganization. Channel response corresponds to the two-phase model of sediment transport and storage proposed by *Lisle and Church* [2002]. Rapid channel incision during winter 2002–2003 corresponds to the transport-limited conditions of phase I. Bed armoring and reduction in incision rate drove channel widening and continued sediment export at the transition to supply-limited conditions of phase II.

4.1. Channel Incision and Lag Formation

[26] We used field observations, channel surveys, and hydrologic data to construct a time series of cumulative channel incision and sediment export at the landslide (Figure 9). Channel incision and the formation of an incipient lag occurred rapidly within the first two months following the landslide. Photographs of the channel taken 25 April 2002 by the U.S. Forest Service (R. Hausinger, personal communication, 2004) document approximately 4–6 m of vertical incision and considerable armoring of the channel bed relative to the undisturbed surface of the landslide. During this brief period, the maximum 24-hour precipitation at Darrington was 76 mm (Figure 2). Photographs taken 25 days later on 20 May 2002 (R. Hausinger, personal communication, 2004) showed no discernable bed lowering based on key boulders in the same orientation as those in the 25 April photographs. Daily precipitation between the April and May 2002 photographs did not exceed the previous maximum precipitation. Field evidence of significant bed reorganization was apparent during our first site visit approximately one year later on 30 May 2003. The earlier 24-hour precipitation maximum of 76 mm was exceeded once (91 mm, 13 March 2003) between the 20 May 2002 photographs and our 30 May 2003 site visit.

[27] The first detailed survey of the channel profile in summer 2003 measured up to 9 m of vertical incision relative to the estimated elevation of the original landslide surface (Table 1). Channel incision prior to the 2003 survey eroded most of the fine sediment from the channel and coarsened the bed relative to the surface of the landslide deposit. The grain size distribution of sediment sampled from the bed of the channel, where it had incised into the landslide, coarsened with increasing shear stress relative to the original landslide particle size distribution (Figure 10). The landslide deposit exhibited a bimodal distribution, which we posit developed during the mixing of rockfall material with entrained colluvium and glacial sediments. The landslide material also had a geometric sorting coefficient (σ_g) of 1.44, where $\sigma_g = (\psi_{84} - \psi_{16})/2$. Results of the 2003 sediment sampling indicate that the median bed surface grain size increased with both the local shear stress and the local incision depth (Figure 11). Dimensionless shear stress (Shields number) calculated for the 11 samples ranged from 0.4 to 0.8. Comparison with a typical range of 0.03–0.06 for incipient motion [*Buffington and Montgomery*, 1997] indicates energy losses of up to about 84–95% during the winter 2002–2003 peak flow. The degree of bed armoring (surface D_{50}/supply D_{50}) ranged from 2.2 to 10.1 (mean of 5.6). On the basis of the interpolation of cross-sectional areas, approximately 22,000 m^3 of sediment (9% of the

Table 1. Results of the Probabilistic Analysis for Summer 2003 Field Conditions

Bed Surface Sample	Profile Distance, m	Incision Depth, m	D_{50}, mm	D_{90}, mm	τ, Pa	τ^*[a]	Model $D[t(s_i) = 0.05]$, mm	Model D_{max}, mm	r^2
f_1	653	1	108	321	665	0.37	405	426	0.89
f_2	635	2	77	301	762	0.59	425	447	0.80
f_3	607	1	131	331	1,049	0.48	475	500	0.70
f_4	423	4	190	538	1,276	0.40	509	535	0.96
f_5	490	4	97	352	1,281	0.79	510	536	0.76
f_6	442	4	120	350	1,329	0.66	517	543	0.66
f_7	469	5	150	502	1,380	0.55	524	550	0.91
f_8	408	6	251	912	2,275	0.54	624	656	0.95
f_9	363	7	374	1,225	2,659	0.43	766	693	0.88
f_{10}	386	9	452	1,060	4,076	0.54	659	806	0.89
f_{11}	337	5	373	1,564	4,722	0.76	807	849	0.85
								total:	0.83

[a]Shields number, $\tau^* = \tau/[g(\rho_s - \rho)D_{50}]$, where ρ_s and ρ are the densities of sediment (2700 kg/m^3) and water (1000 kg/m^3), respectively, and τ is the total shear stress not accounting for losses from hydraulic roughness. See text for explanation.

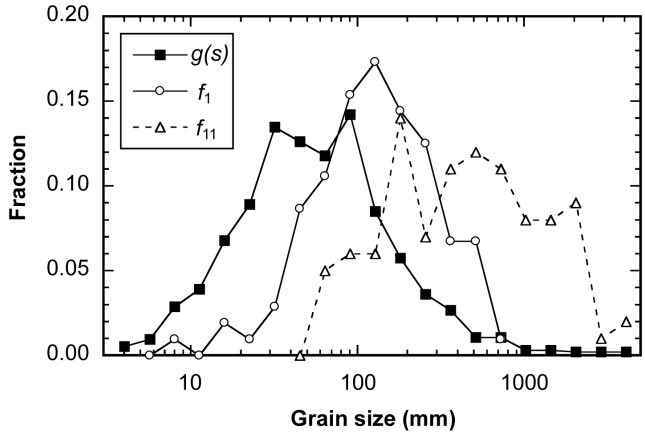

Figure 10. Variation in grain size distribution of sediment supplied by the landslide ($g(s)$) and two representative sample locations from the bed surface of the channel. Bed surface distribution coarsens relative to the supply with increasing shear stress from f_1 to f_{11} (see Table 1).

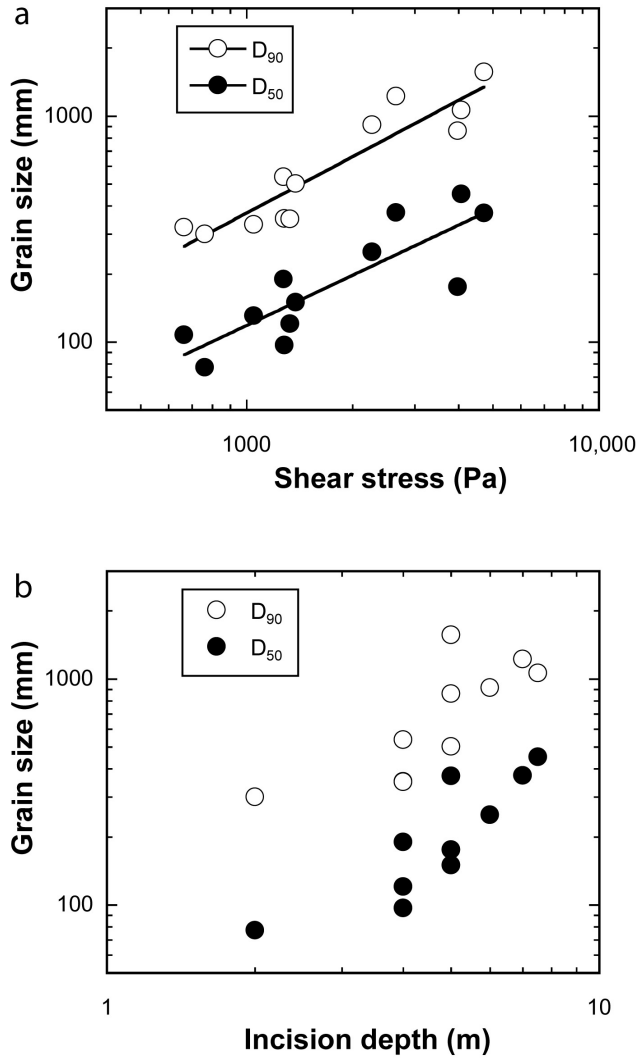

Figure 11. Variation in bed surface grain size versus (a) total shear stress and (b) incision depth.

estimated original landslide volume within the valley bottom and available for channel reworking) was eroded from the landslide during the latter half of winter 2001–2002 and through winter 2002–2003.

[28] Runoff generated by several high-intensity storms between 16–21 October 2003 resulted in significant channel adjustment at the study site and caused local flooding and property damage throughout the region. Although Squire Creek was not gauged at the time, the recurrence interval of October 2003 floods on six nearby gauged rivers ranged from 8 to 152 years. The Darrington Ranger Station recorded 417 mm of precipitation during this 6-day period. The maximum 24-hour precipitation from the prior rainy season was exceeded twice during this period (141 mm and 155 mm). A resurvey of the channel thalweg and cross sections following the intense October 2003 storms documented minor vertical change in the profile, but considerable bank erosion and channel widening. The maximum vertical change in local thalweg elevation measured among the nine cross sections between the 2003 and 2004 surveys was 1.9 m and only slightly greater than the vertical precision of the survey set by the D_{90} of the bed ($\sim$1 m). However, bank retreat eroded an additional 26,000 m^3 of sediment (11% of the original landslide volume) and increased the local channel width by up to 27 m. Bank migration into the adjacent forest downstream of cross section 4 (station 419) exhumed stored sediment from the prehistoric landslide deposit. Although the channel was not resurveyed until summer 2004 when flows receded, periodic site visits and photo documentation showed no evidence of bed reorganization between the October 2003 storms and the 2004 survey. Likewise, comparison of the 2004 and 2005 surveys showed no significant (>1 m) change in cross sections or profile. The peak 24-hour precipitation recorded between the October 2003 storms and the summer 2004 survey was 80 mm, which is less than the 2002–2003 maximum, but greater than the peak 24-hour precipitation recorded in April 2002. The maxi-

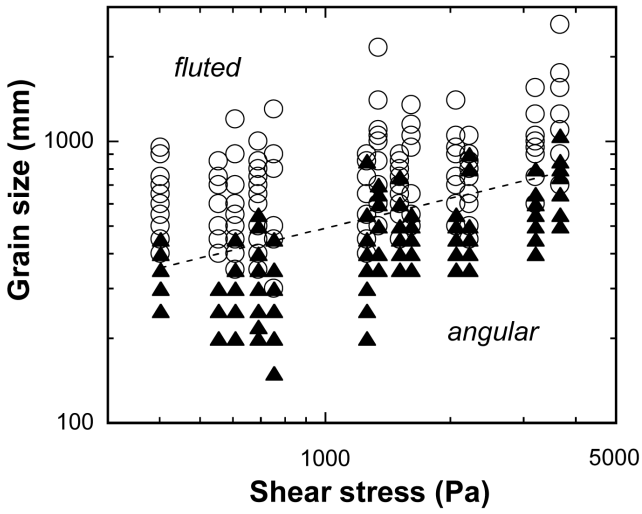

Figure 12. Discriminant function (dashed line: $D = 43\ \tau^{0.35}$, $r^2 = 0.69$) defining relation between the grain size of fluted (stable) and angular (mobile) clasts measured during the tracer study downstream of the landslide dam.

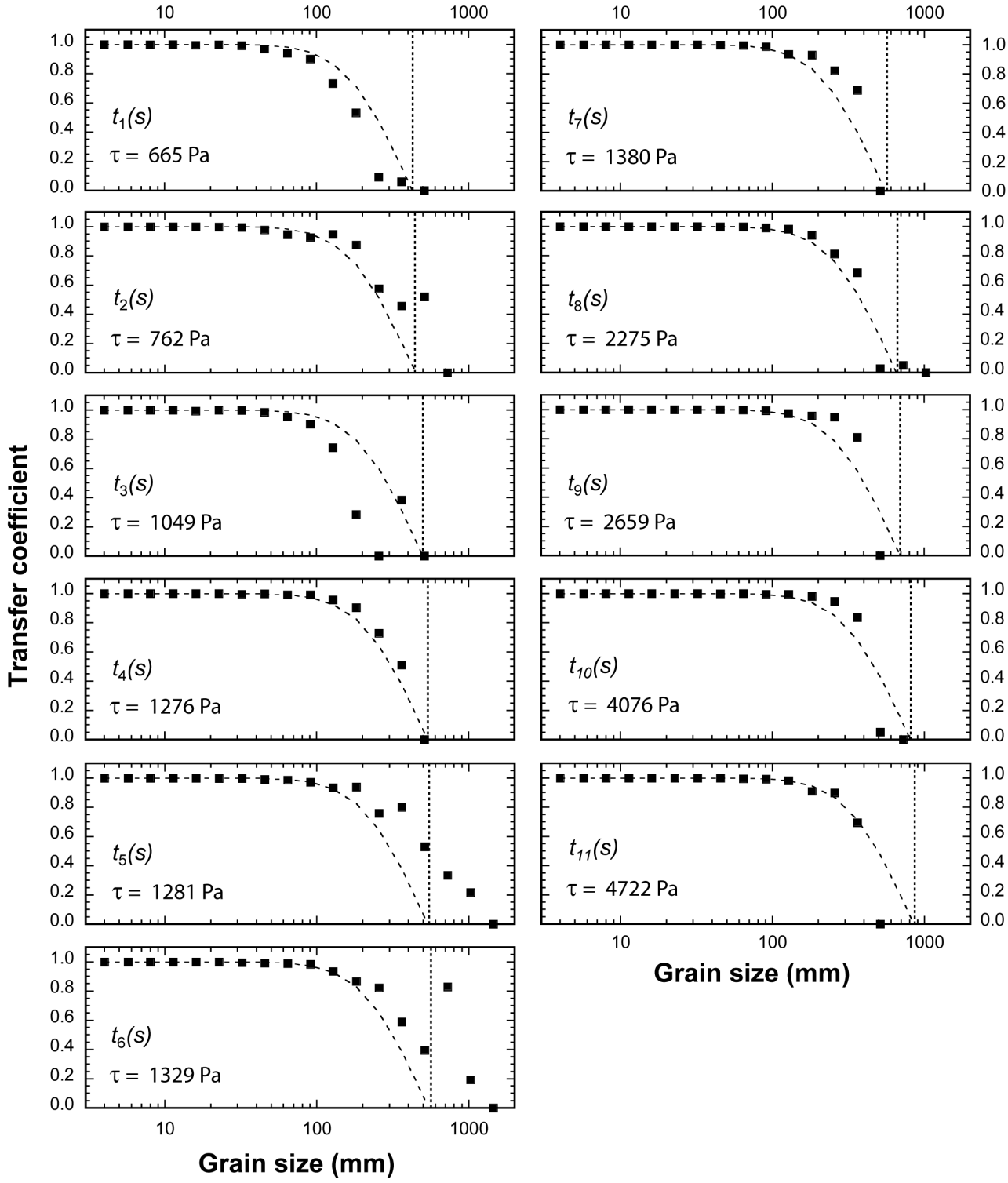

Figure 13. Semilog plots of transfer coefficients versus grain size calculated from equation (10) for the 11 sample locations. Dashed lines are the general solution for transfer functions (equation (14)), and vertical dotted lines denote D_{max}.

mum 24-hour precipitation at Darrington between the 2004 and 2005 surveys was 118 mm on 9 December 2004, which triggered the peak discharge for the season of 126 m^3/sec on 10 December 2004.

4.2. Tracer Study

[29] The intermediate diameter of fluted and potholed particles sampled downstream of the landslide in 2003 was significantly greater than the diameter of angular particles

(Figure 12). The best fit relation that discriminates between groups of stable and mobile sediment sizes is positively correlated with total shear stress ($r^2 = 0.69$). The discriminant function derived from results of the tracer study is given by

$$D = 43\tau^{0.35} \tag{11}$$

where D is the particle diameter in mm that best discriminates between stable and mobile clasts and τ is the total shear stress in Pa, as defined earlier. Grain sizes from which equation (11) was derived ranged from 350–760 mm over a range of total shear stress of 400–3670 Pa.

4.3. Probabilistic Model

[30] The transfer functions calculated from equation (10) display the same general form for all 11 sample locations (Figure 13). The asymptotic behavior toward unity for the fine and intermediate grain size intervals indicates that all of the sediment within these size intervals was eroded during channel incision. The decay in transfer coefficients over the coarsest four to five grain size intervals indicates a decline in the proportion of coarse sediment removed from the deposit during incision and an increase in the proportion of coarse sediment remaining to form a stable bed surface. In most cases, the intervals comprising the coarse tails of the distributions, where transfer coefficients are noticeably <1, show the greatest variability between transfer coefficients. The variability is attributed to the small sample sizes within the coarsest size intervals. The transfer functions also become increasingly skewed toward coarser size intervals with increasing shear stress.

[31] The slope and intercept of the discriminant function derived from the tracer study (equation (11)) roughly correspond to the maximum mobile grain size (D_{max}) inferred from the field-based transfer coefficients (Figure 13), even though the size of some angular (i.e., mobile) particles sampled in the tracer study fall above the discriminant line in Figure 12. This may be due to the relatively low form roughness of the ambient bed (from which tracer particles were collected) in comparison to bed conditions of the highly armored channel passing through the landslide deposit. Equation (11) was therefore used to derive a general solution for the transfer function by incorporating the power law regression between total shear stress and grain size into the error function (erf):

$$t(s) = \mathrm{erf}\left[c \log_2 \left(\frac{a\tau^b}{D_i}\right)\right] \tag{12}$$

where c is a shape factor that scales the grain size range over which $t(s)$ decays from near unity to zero. The error function is defined by

$$\mathrm{erf}(x) = \frac{2}{\sqrt{\pi}} \int_0^x e^{-u^2} du \tag{13}$$

[32] We substituted the coefficient and exponent derived from the discriminant analysis (equation (11)) for a and b in equation (12) and then solved for c by minimizing the sum of the squares of the residuals for the ensemble of field data. In doing so, the numerator in the log expression is explicitly set equal to D_{max}. The general solution for the transfer function is then given by

$$t(s) = \mathrm{erf}\left[0.61 \log_2 \left(\frac{43\tau^{0.35}}{D_i}\right)\right] \tag{14}$$

Equation (14) provides a satisfactory fit (composite $r^2 = 0.84$) to the ensemble of transfer functions (Figure 13 and Table 1). Solving for D_i of the bed material in equation (14) when $t(s)$ equals 0.95 (when 5% of D_i particles are immobile) indicates that transfer coefficients begin diverging from unity at a threshold given by

$$D_i = 9.0\tau^{0.35} \tag{15}$$

Because the transfer coefficients are undefined for negative values, $t(s)$ was set equal to zero for the condition

$$D_i > 43\tau^{0.35} \tag{16}$$

[33] Equations (15) and (16) define the grain size range over which the transfer function decays from unity to zero assuming a homogeneous supply distribution. However, mechanical sorting by the landslide and topographic focusing of the landslide trajectory during transport to the valley floor may have introduced spatial variability in the supply distribution. In such cases, the general solution may diverge from the field-based transfer function. Local variability in $G_n(s)$ and $t_n(s)$ may also occur when the incision depth is less than the size of the largest particles in the supply distribution; examples of such variability are presented in Figure 13 for $t_1(s)$, $t_2(s)$, and $t_3(s)$, where the incision depths were limited to 1–2 m.

4.4. Bed Shielding and Step-Pool Formation

[34] The fraction of the bed surface covered by relatively immobile particles in summer 2003 was evaluated using the general solution for the transfer function (equation (14)). Lag boulders (D with <5% probability of entrainment prior to the October 2003 storms) covered 8–30% (average of 20%) of the bed surface through the most deeply incised portion of the landslide (Table 1). The degree of armoring was relatively high and as much as 5 times greater than the armoring measured for the finer-grained sediment pulse investigated by *Sutherland et al.* [2002]. A comparison of the median step-forming grain size with the grain size corresponding to a transfer coefficient of 0.05 indicates that all of the steps we sampled were formed by lag boulders with a <5% probability of entrainment (Figure 14a). An additional comparison of the median step-forming grain size with the reach average D_{90} of the bed surface indicates that most lag boulders fell within the upper 10th percentile of the bed surface grain size distribution (Figure 14b).

[35] Minor vertical incision (locally <2 m) and significant channel widening of up to 27 m occurred during the storms of October 2003 (Figure 7). Alternating bank erosion during channel widening in October 2003 increased the thalweg sinuosity, which is illustrated in the cross sections by alternating bank erosion from the left bank (cross sections 1–4) to the right bank (cross sections 5–8) and then back to left bank (cross sections 8 and 9). The increase in sinuosity effectively reduced the channel gradient by increasing the

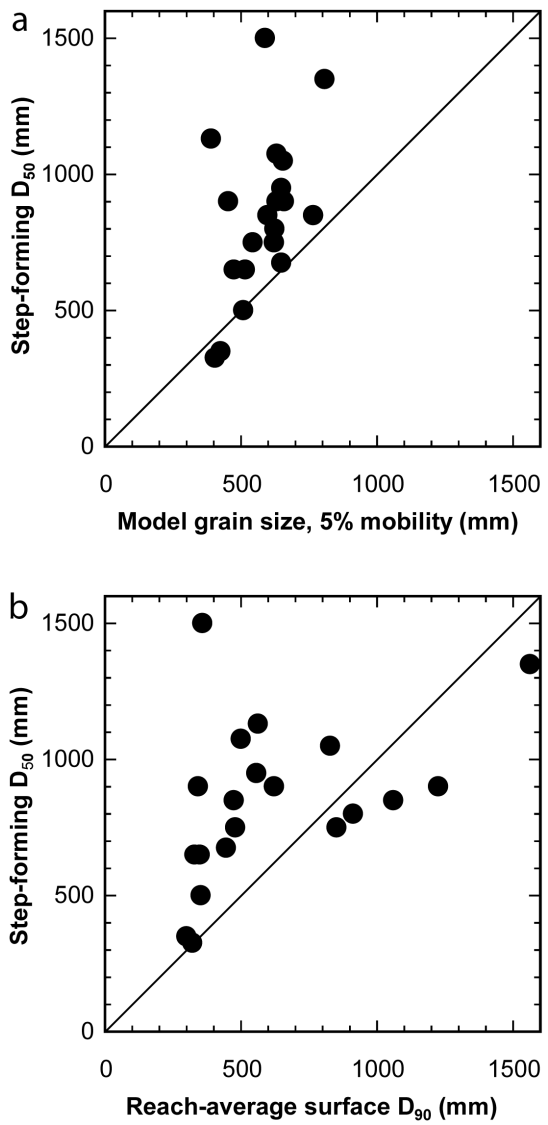

Figure 14. Plots of the median grain size of step-forming boulders versus (a) the model grain size with a 5% mobility and (b) the reach average, bed surface D_{90}.

thalweg length through the deposit (the 2004 profile was constructed along the high-flow alignment, which has a lower sinuosity).

5. Discussion

[36] Higher local shear stress along the steepest reach of the new channel drove deeper incision of the landslide deposit over the negative feedback of armoring and coarsened the bed relative to the original particle size distribution. Vertical incision declined rapidly as the bed surface armored with a lag of relatively immobile particles. The decline in the value of transfer coefficients (or the probability of mobilization) at the coarse tail of the 11 grain size distributions (Figure 13) indicates that lag formation was driven by the selective transport of fine material from the poorly sorted landslide deposit. The characteristic form of the transfer functions shows that all particle sizes were not mobilized equally relative to their individual fractions present within the sediment pulse. Our findings are consistent with those of *Lisle* [1995], who found that selective transport was most prevalent in steep, coarse-bedded channels, where annual bed scour did not regularly penetrate below the armor layer. In a similar study of fluvial recovery at Mount Pinatubo, *Gran and Montgomery* [2005] found that a seasonal decline in sediment supply during the dry season, combined with selective transport of fine material from the bed, drove vertical incision and bed armoring, which increased form drag and inhibited bed mobility. Our findings suggest that selective transport may be widespread throughout mountain channel networks and dominate the reworking of nonfluvial sediment supplied to confined channels.

[37] Lag formation also involved the organization of the coarsest particles into energy-dissipating steps that apparently limited scour during the October 2003 event and shielded the bed from further incision. The largest boulders provided stable nuclei for step formation. Our results show that a grain size percentile coarser than the conventional D_{50} (such as D_{90}) may be the appropriate reference grain size in steep, confined mountain channels, where bed reorganization of step-pool structures is controlled by the mobility threshold of the largest step-forming clasts [*Grant et al.*, 1990; *Lenzi*, 2001; *Madej*, 2001; *Kasai et al.*, 2004; *Chin and Wohl*, 2005].

[38] The chronology of channel incision reconstructed from photographs and channel surveys indicates that reworking of the bed by progressively larger flows during lag formation increased the threshold for further bed reorganization and forced the channel to widen during the high-magnitude flood of October 2003. We interpret the observed channel widening to indicate a shift in the process of sediment pulse dispersion from vertical incision to lateral erosion, a process change expected to follow bed stabilization by a relatively immobile lag. Channel widening and the increase in sinuosity caused by local variations in lateral migration further stabilized the bed. Channel widening decreased the flow depth and tractive forces acting on the bed by future flows of lesser magnitude than the October 2003 event. Likewise, the increase in sinuosity effectively reduced the channel gradient by increasing the channel length through the landslide.

[39] Our findings that armor formation limits vertical incision and forces channel widening are consistent with previous studies of debris fan erosion in the canyon rivers of the Colorado Plateau. *Pizutto et al.* [1999] and *Webb et al.* [1999] monitored the effects of the controlled flood of 1996 in the Grand Canyon and found that previous armoring of debris fan surfaces by several small-magnitude floods inhibited significant reworking in 1996, whereas recently aggraded fans exhibited the greatest amount of reworking. *Larsen et al.* [2004] also reported limited reworking of previously armored debris fans by successive floods of comparable magnitude in a similar study along the Green River of Colorado and Utah. Previous studies within canyon rivers found that lateral erosion was the most significant mechanism of debris fan dispersion [*Kieffer*, 1985; *Hammack and Wohl*, 1996; *Pizzuto et al.*, 1999; *Webb et al.*, 1999; *Larsen et al.*, 2004]. *Pizzuto et al.* [1999] reported that reworking of a coarse-grained debris fan during the 1996 controlled flood ended after four hours, when large

boulders armored the unconsolidated banks. Similarly, we also observed armoring at the base of the banks of Squire Creek (Figure 8). In contrast, *Hammack and Wohl* [1996] suggested, on the basis of hydraulic modeling along a debris fan in the Yampa River, that erosion may continue in the portions already widened by previous, higher-magnitude flows. These authors showed that the critical shear stress for entrainment of the largest particles in the Yampa River debris fan is exceeded even during the 1-year recurrence flow and suggested that the duration of flows may be as important as flow magnitude for the dispersion of sediment pulses not dominated by the coarse tail of the grain size distribution.

[40] Results of the probabilistic model of particle entrainment provide insights on possible constraints for lag formation and channel widening. Our results suggest that a poorly sorted sediment pulse must contain a sufficient concentration and caliber of coarse particles that are not readily mobilized during high-magnitude flows in order to form a relatively stable armor and the energy-dissipating structures capable of significantly retarding vertical incision into the deposit. This is consistent with other field studies showing the longevity of poorly sorted debris flows containing large boulders [*Miller and Benda*, 2000; *Benda et al.*, 2003; *Korup*, 2005; *Korup et al.*, 2006]. The erosivity of the supply lithology may provide an additional control on the long-term dispersion rate of sediment pulses [*Nolan and Marron*, 1985; *Taylor and Kite*, 2006]. Because armoring develops rapidly during low-magnitude flows, lag deposits can shield sediment pulses and sequester large volumes of sediment in mountain channel networks over time periods exceeding the recurrence of characteristic bed-reorganizing events. Hence lag deposits can attenuate the downstream delivery of sediment introduced by large-scale disturbances and should be common in confined mountain channels prone to coarse-grained sediment inputs from bedrock slopes that supply material resilient against mechanical weathering by fluvial erosion.

[41] We hypothesize that the relict lag boulders and profile convexities mapped elsewhere along Squire Creek and observed throughout similar mountain drainage basins in the Pacific Northwest record bed armoring and profile stabilization that may play a more significant role in retarding the decay of coarse-grained sediment pulses than previously recognized. In particular, the persistence of such deposits has implications for how coarse-grained debris dams function as large sediment "capacitors" in mountain channels by moderating sediment flux through the charging and discharging of sediment reservoirs. Our case study fits the two-phase model of degrading, gravel bed channels proposed by *Lisle and Church* [2002] and provides a field-based measure of the timescale for phase I, which is 1–2 years. Our results show that channel widening immediately after profile stabilization by a persistent armor layer may prolong the initial period of high sediment export. Consequently, numerical models of sediment pulse evolution that do not explicitly incorporate the linkages between lag formation and lateral erosion may underestimate dispersion during channel widening by these end-member, coarse-grained sediment pulses but later overestimate dispersion once a lag forms. Hence the grain size distribution and lithology of a sediment input relative to the flow competence of the receiving channel appear to be critical factors influencing the rates and mechanisms of sediment pulse dispersion in mountain drainage basins.

6. Conclusions

[42] Results from a 4-year field study of a valley-spanning landslide document the effects of a persistent armor layer on the incision and reworking of a poorly sorted sediment pulse containing a significant fraction of particles not readily transported as bed load by high-magnitude flows. Rapid bed surface armoring of the recovering channel was driven by selective transport during moderate-intensity flows in 2002 and 2003. Bed shielding by an incipient lag inhibited bed scour and forced the channel to widen during the October 2003 high-magnitude flood. Despite a decrease in vertical incision, widening in 2003 eroded more sediment than during all the previous reworking events combined. Lag boulders with <5% probability of entrainment and exceeding the reach average D_{90} covered an average of 20% of the bed surface and comprised most of the step-forming clasts. The long residence time of exceptionally large particles and persistence of lag deposits have implications for how coarse-grained debris dams function as large sediment capacitors in mountain channels confined by steep valley slopes prone to landsliding.

[43] **Acknowledgments.** This research was supported by grants from the USDA Pacific Northwest Research Station and the University of Washington, Department of Earth and Space Sciences. We thank Bretwood Higman for assistance with the MB model. We also acknowledge the contributions of Ron Hausinger, Bob Norris, Thom Davis, and David Luzi. We thank Erik Blumhagen, Jeremy Bunn, Lisa Good-Brummer, Laura Hughes, Michael Lamb, Sadie Rosenthal, and Peter Wald for their assistance in the field. Tom Lisle, Ellen Wohl, and an anonymous reviewer provided helpful reviews of an earlier draft.

References

Abrahams, A. D., G. Li, and J. F. Atkinson (1995), Step-pool streams: Adjustment to maximum flow resistance, *Water Resour. Res.*, *31*, 2593–2602.

Andrews, E. D. (1980), Effective and bankfull discharges in the Yampa basin, Colorado and Wyoming, *J. Hydrol.*, *46*, 311–330.

Benda, L. E. (1990), The influence of debris flows on channels and valley floors in the Oregon Coast Range, U.S.A., *Earth Surf. Processes Landforms*, *15*, 457–466.

Benda, L. E., C. Veldhuisen, and J. Black (2003), Debris flows as agents of morphological heterogeneity at low-order confluences, Olympic Mountains, Washington, *Geol. Soc. Am. Bull.*, *115*, 1110–1121.

Brummer, C. J., and D. R. Montgomery (2003), Downstream coarsening in headwater channels, *Water Resour. Res.*, *39*(10), 1294, doi:10.1029/2003WR001981.

Buffington, J. M., and D. R. Montgomery (1997), A systematic analysis of eight decades of incipient motion studies, with special reference to gravel-bedded rivers, *Water Resour. Res.*, *33*, 1993–2029.

Buffington, J. R., and D. R. Montgomery (1999), Effects of sediment supply on surface textures of gravel-bed rivers, *Water Resour. Res.*, *35*, 3523–3530.

Caine, N., and F. J. Swanson (1989), Geomorphic coupling of hillslope and channel systems in two small mountain basins, *Z. Geomorphol.*, *33*, 189–203.

Chartrand, S. M., and P. J. Whiting (2000), Alluvial architecture in headwater streams with special emphasis on step-pool topography, *Earth Surf. Processes Landforms*, *25*, 583–600.

Chin, A., and E. Wohl (2005), Toward a theory for step pools in stream channels, *Prog. Phys. Geogr.*, *29*, 275–296.

Church, M., M. A. Hassan, and J. F. Wolcott (1998), Stabilizing self-organized structures in gravel-bed stream channels: Field and experimental observations, *Water Resour. Res.*, *34*, 3169–3179.

Costa, J. E., and R. L. Schuster (1991), Documented historical landslide dams from around the world, *U.S. Geol. Surv. Open File Rep.*, *91-239*, 486 pp.

Cui, Y., G. Parker, T. E. Lisle, J. Gott, M. W. Hansler-Ball, J. E. Pizzuto, N. E. Allmendinger, and J. M. Reed (2003a), Sediment pulses in mountain rivers: 1. Experiments, *Water Resour. Res.*, *39*(9), 1239, doi:10.1029/2002WR001803.

Cui, Y., G. Parker, J. E. Pizzuto, and T. E. Lisle (2003b), Sediment pulses in mountain rivers: 2. Comparison between experiments and numerical predictions, *Water Resour. Res.*, *39*(9), 1240, doi:10.1029/2002WR001805.

Curran, J. C., and P. R. Wilcock (2005), The characteristic dimensions of the step-pool bed configuration: An experimental study, *Water Resour. Res.*, *41*, W02030, doi:10.1029/2004WR003568.

Daly, C., and G. Taylor (1998), Washington average annual precipitation (1961–1990), report, Oreg. Clim. Serv., Oreg. State Univ., Corvallis.

Dietrich, W. E., and T. Dunne (1978), Sediment budget for a small catchment in mountainous terrain, *Z. Geomorphol.*, *29*, 191–206.

Dietrich, W. E., J. W. Kirchner, H. Ikeda, and F. Iseya (1989), Sediment supply and the development of the coarse surface layer in gravel-bedded rivers, *Nature*, *340*, 215–217.

Gilbert, G. K. (1917), Hydraulic mining debris in the Sierra Nevada, *U.S. Geol. Surv. Prof. Pap., 105*, 154 pp.

Gran, K. B., and D. R. Montgomery (2005), Spatial and temporal patterns in fluvial recovery following volcanic eruptions: Channel response to basin-wide sediment loading at Mount Pinatubo, Philippines, *Geol. Soc. Am. Bull.*, *117*, 195–211.

Grant, G. E. (1997), Critical flow constrains flow hydraulics in mobile-bed streams: A new hypothesis, *Water Resour. Res.*, *33*, 349–358.

Grant, G. E., F. J. Swanson, and M. G. Wolman (1990), Pattern and origin of stepped-bed morphology in high-gradient streams, western Cascades, Oregon, *Geol. Soc. Am. Bull.*, *102*, 340–352.

Hammack, L., and E. Wohl (1996), Debris-fan formation and rapid modification at Warm Springs Rapid, Yampa River, Colorado, *J. Geol.*, *104*, 729–740.

Kasai, M., T. Marutani, and G. Brierley (2004), Channel bed adjustment following major aggradation in a steep headwater setting: Findings from Oyabu Creek, Kyushu, Japan, *Geomorphology*, *62*, 199–215.

Kieffer, S. W. (1985), The 1983 hydraulic jump in Crystal Rapid: Implications for river-running and geomorphic evolution in the Grand Canyon, *J. Geol.*, *93*, 385–406.

Kinerson, D. (1990), Surface response to sediment supply, M.S. thesis, Univ. of Calif., Berkeley.

Korup, O. (2004), Landslide-induced river channel avulsions in mountain catchments of southwest New Zealand, *Geomorphology*, *63*, 57–80.

Korup, O. (2005), Geomorphic hazard assessment of landslide dams in South Westland, New Zealand: fundamental problems and approaches, *Geomorphology*, *66*, 167–188.

Korup, O., A. L. Strom, and J. T. Weidinger (2006), Fluvial response to large rocks-slope failures: Examples from the Himalayas, the Tien Shan, and the Southern Alps in New Zealand, *Geomorphology*, in press.

Larsen, I. J., J. C. Schmidt, and J. A. Martin (2004), Debris-fan reworking during low-magnitude floods in the Green River canyons of the eastern Uinta Mountains, Colorado and Utah, *Geol.*, *32*, 309–312.

Lenzi, M. A. (2001), Step-pool evolution in the Rio Cordon, northeastern Italy, *Earth Surf. Processes Landforms*, *26*, 991–1008.

Leopold, L. B., M. G. Wolman, and J. P. Miller (1964), *Fluvial Processes in Geomorphology*, W.H. Freeman, New York.

Lisle, T. E. (1995), Particle size variations between bed load and bed material in natural gravel bed channels, *Water Resour. Res.*, *31*, 1107–1118.

Lisle, T. E., and M. Church (2002), Sediment transport-storage relations for degrading, gravel bed channels, *Water Resour. Res.*, *38*(11), 1219, doi:10.1029/2001WR001086.

Lisle, T. E., J. E. Pizzuto, H. Ikeda, F. Iseya, and Y. Kodama (1997), Evolution of a sediment wave in an experimental channel, *Water Resour. Res.*, *33*, 1971–1981.

Madej, M. A. (2001), Development of channel organization and roughness following sediment pulses in single-thread, gravel bed rivers, *Water Resour. Res.*, *37*, 2259–2272.

Madej, M. A., and V. Ozaki (1996), Channel response to sediment wave propagation and movement, Redwood Creek, California, USA, *Earth Surf. Processes Landforms*, *21*, 911–927.

McLaren, P., and D. Bowles (1985), The effects of sediment transport on grain-size distributions, *J. Sediment. Petrol.*, *55*, 457–470.

Miller, D. J., and L. E. Benda (2000), Effects of punctuated sediment supply on valley-floor landforms and sediment transport, *Geol. Soc. Am. Bull.*, *112*, 1814–1824.

Montgomery, D. R., and J. M. Buffington (1997), Channel reach morphology in mountain drainage basins, *Geol. Soc. Am. Bull.*, *109*, 596–611.

Nolan, K. M., and D. C. Marron (1985), Contrast in stream-channel response to major storms in two mountainous areas of California, *Geology*, *13*, 135–138.

Ouimet, W. B., and K. X. Whipple (2004), Mega-landslides in eastern Tibet: Implications for landscape and river profile evolution, and the interpretation of tectonics from topography, *Eos Trans. AGU*, *85*(47), Fall Meet. Suppl., Abstract H44A-04.

Perkins, S. J. (1989), Interactions of landslide-supplied sediment with channel morphology in forested watersheds, M.S. thesis, Univ. of Wash., Seattle.

Pizzuto, J. E., R. H. Webb, P. G. Griffiths, J. G. Elliott, and T. S. Melis (1999), Entrainment and transport of cobbles and boulders from debris fans, in *The Controlled Flood in Grand Canyon*, *Geophys. Monogr. Ser.*, vol. 110, edited by A. B. Jones, pp. 53–70, AGU, Washington, D. C.

Pringle, P. T., R. L. Schuster, and R. L. Logan (1998), New radiocarbon ages of major landslides in the Cascade Range, Washington, *Wash. Geol.*, *26*, 31–39.

Roberts, R. G., and M. C. Church (1987), The sediment budget in severely disturbed watersheds, Queen Charlotte Ranges, British Columbia, *Can. J. For. Res.*, *16*, 1092–1106.

Schumm, S. A. (1963), Sinuosity of alluvial rivers on the Great Plains, *Geol. Soc. Am. Bull.*, *74*, 1000–1089.

Schuster, R. L., R. L. Logan, and P. T. Pringle (1992), Prehistoric rock avalanches in the Olympic Mountains, Washington, *Science*, *258*, 1620–1621.

Springer, G. S., S. Tooth, and E. E. Wohl (2005), Dynamics of pothole growth as defined by field data and geometrical description, *J. Geophys. Res.*, *110*, F04010, doi:10.1029/2005JF000321.

Sutherland, A. J. (1987), Static armour layers by selective erosion, in *Sediment Transport in Gravel-Bed Rivers*, edited by C. R. Thorne, J. C. Bathurst, and R. D. Hey, pp. 243–267, John Wiley, Hoboken, N. J.

Sutherland, D. G., M. W. Hansler-Ball, S. J. Hilton, and T. L. Lisle (2002), Evolution of a landslide-induced sediment wave in the Navarro River, California, *Geol. Soc. Am. Bull.*, *114*, 1036–1048.

Tabor, R. W., D. B. Booth, J. A. Vance, and A. B. Ford (2002), Geologic map of the Sauk River 30′ by 60′ quadrangle, Washington, *U. S. Geol. Surv. Misc. Invest. Map, I-2592*, scale 1:100000, 2 sheets, 64 pp.

Taylor, S. B., and J. S. Kite (2006), Comparative geomorphic analysis of surficial deposits at three Appalachian watersheds: Implications for controls on sediment-transport efficiency, *Geomorphology*, in press.

Webb, R. H., T. S. Melis, P. G. Griffiths, and J. G. (1999), Reworking of aggraded debris fans, in *The Controlled Flood in Grand Canyon*, *Geophys. Monogr. Ser.*, vol. 110, edited by A. B. Jones, pp. 37–51, AGU, Washington, D. C.

Whipple, K. X., G. S. Hancock, and R. S. Anderson (2000), River incision into bedrock: Mechanics and relatively efficacy of plucking, abrasion, and cavitation, *Geol. Soc. Am. Bull.*, *112*, 490–503.

Whiting, P. J., J. F. Stamm, D. B. Moog, and R. L. Orndorff (1999), Sediment transporting flows in headwater channels, *Geol. Soc. Am. Bull.*, *111*, 450–466.

Whittaker, J. G., and M. N. R. Jaeggi (1982), Origin of step-pool systems in mountain streams, *J. Hydraul. Div. Am. Soc. Civ. Eng.*, *108*, 99–104.

Wohl, E., and D. A. Cenderelli (2000), Sediment deposition and transport patterns following a reservoir sediment release, *Water Resour. Res.*, *36*, 319–333.

Wolman, M. G. (1954), A method of sampling coarse river-bed material, *Eos Trans. AGU*, *35*, 951–956.

Wolman, M. G., and J. Miller (1960), Magnitude and frequency of forces in geomorphic processes, *J. Geol.*, *69*, 54–74.

Zimmerman, A., and M. C. Church (2001), Channel morphology, gradient profiles and bed stresses during flood in a step-pool channel, *Geomorphology*, *40*, 311–327.

C. J. Brummer and D. R. Montgomery, Department of Earth and Space Sciences, Box 351310, University of Washington, Seattle, WA 98195, USA. (cbrummer@u.washington.edu)